1384 *Inorg. Chem.* **2010**, *49*, 1384–1396
DOI: 10.1021/ic9014515

Inorganic Chemistry
Article

Searching for the Interlayer Band and Unravelling the Bonding in β-$ThSi_2$ and α-$ThSi_2$ with *N*MTO Wannier-like Functions

Eva Zurek,*,† Ove Jepsen, and Ole Krogh Andersen*

Max-Planck-Institut für Festkörperforschung, Heisenbergstrasse 1, 70569, Stuttgart, Germany. †Current address: Department of Chemistry, State University of New York at Buffalo, Buffalo, New York 14260-3000

Received July 22, 2009

Using the newly developed *N*MTO (muffin-tin orbitals of order *N*) technique, which generates atom-centered, localized, Wannier-like functions, we investigate whether—such as in graphites—an interlayer band exists at the Fermi level in $ThSi_2$ with six electrons per Si. We find that the Th s-like *N*MTO, not only in the graphite-structured β-$ThSi_2$ but also in the twisted allotrope, α-$ThSi_2$, strikingly resembles the previously calculated interlayer *N*MTO in graphites and that the corresponding band cuts the Fermi level but is at many places gapped, particulaly in the twisted allotrope. This suggests that the mechanism of superconductivity in both allotropes of $ThSi_2$ is similar to the one in intercalated graphites such as CaC_6 with $4^1/_3$ electrons per C. Here, C buckling and Ca in-plane phonons couple between interlayer and π^* bands. In $ThSi_2$, not only these bands but also the σ^* band cross the Fermi level, and intraband coupling via Si bond-stretching modes, like in MgB_2, is likely to contribute to the superconductivity. Finally, we investigate the bonding in $ThSi_2$ by seeking those *N*MTO basis sets with merely nine or six orbitals per $ThSi_2$, which best span the occupied bands. Our results indicate that in both allotropes there are three weakened Si−Si σ bonds, two Th−Si sp_z bonds, and a nonbonding Si p_z-orbital.

1. Introduction

Since the discovery of superconductivity in MgB_2[1] much effort has been spent on studies of sp^2-bonded intercalated graphites and structurally related compounds.[2−5] With four electrons per boron, MgB_2 is isoelectronic with graphite but is unique in having intercalated doubly charged ions lower the energy of the boron π bands, to the extent that holes occur at the top of the sp^2-bonding σ bands. As first suggested by density-functional calculations, it is the strong coupling between these holes via the optical bond-stretching modes which causes superconductivity with $T_c = 40$ K.[6−8]

Whereas MgB_2 may thus be viewed as heavily hole-doped graphite, CaC_6, YbC_6, and Ca(AlSi), with $4^1/_3$ and 4.5 electrons per C or Al/Si, respectively, are heavily electron-doped graphites with carriers in the ubiquitous interlayer band, which lies well above the σ bands and crosses the p_z-antibonding π^* band. Numerous theoretical works have considered the role of the interlayer band.[9−11] This band exists even without intercalation, that is, in primitive graphite, C_2,[12] where the interlayer Wannier function "fills" the hexagonal hole between the graphene layers and is roughly ellipsoidal, oblate, or prolate depending on c/a.[13] The intercalation in CaC_6 is in every third hole, and the interlayer band therefore splits into three sub-bands, of which the lowest crosses the Fermi level. The Wannier function of that band is Ca-centered, and since it spills into the neighboring hexagonal holes free of Ca, it is disk-shaped. It has Ca extended-s character plus some Ca $3d_{3z^2-1}$ character, causing a sign change near the center of the disk. The Wannier function is thus shaped like a torus confined between the graphene layers.[13,14] Since it does not change sign upon 6-fold rotation around the axis, connecting the centers of the two

*To whom correspondence should be addressed. E-mail: ezurek@buffalo.edu (E.Z.), oka@fkf.mpg.de (O.K.A.).

(1) Nagamatsu, J.; Nakagawa, N.; Muranaka, T.; Zenitani, Y.; Akimitsu, J. *Nature* **2001**, *410*, 63.
(2) Weller, T. E.; Ellerby, M.; Saxena, S. S.; Smith, R. P.; Skipper, N. T. *Nat. Phys.* **2005**, *1*, 39.
(3) Emery, N.; Hérold, C.; d'Astuto, M.; Garcia, V.; Bellin, C.; Mareché, J. F.; Lagrange, P.; Loupias, G. *Phys. Rev. Lett.* **2005**, *95*, 087003.
(4) Imai, M.; Sadki, E. H. S.; Abe, H.; Nishida, K.; Kimura, T.; Sato, T.; Hirata, K.; Kitazawa, H. *Phys. Rev. B* **2003**, *68*, 064512.
(5) Sanfilippo, S.; Elsinger, H.; Nùnez-Regueiro, M.; Laborde, O.; LeFloch, S.; Affronte, M.; Olcese, G. L.; Palenzona, A. *Phys. Rev. B* **2000**, *61*, 3800.
(6) Kortus, J.; Mazin, I. I.; Belashchenko, K. D.; Antropov, V. P.; Boyer, L. L. *Phys. Rev. Lett.* **2001**, *86*, 4656.
(7) An, J. M.; Pickett, W. E. *Phys. Rev. Lett.* **2001**, *86*, 4366.
(8) Kong, Y.; Dolgov, O. V.; Jepsen, O.; Andersen, O. K. *Phys. Rev. B* **2001**, *64*, 020501.
(9) Calandra, M.; Mauri, F. *Phys. Rev. Lett.* **2005**, *95*, 237002.
(10) Mazin, I. I. *Phys. Rev. Lett.* **2005**, *95*, 227001.
(11) Csányi, G.; Littlewood, P. B.; Nevidomskyy, A. H.; Pickard, C. J.; Simons, B. D. *Nat. Phys.* **2005**, *1*, 42–45.
(12) Giantomassi, M.; Boeri, L.; Bachelet, G. B. *Phys. Rev. B* **2005**, *72*, 224512.
(13) Boeri, L.; Bachelet, G. B.; Giantomassi, M.; Andersen, O. K. *Phys. Rev. B* **2007**, *76*, 064510.
(14) Mazin, I. I.; Boeri, L.; Dolgov, O. V.; Golubov, A. A.; Bachelet, G. B.; Giantomassi, M.; Andersen, O. K. *Physica C* **2007**, *116*, 460–462.

 Published on Web 01/12/2010

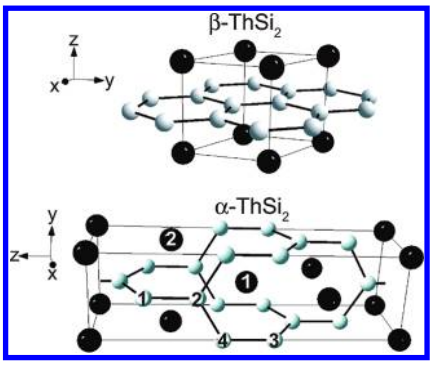

Figure 1. The primitive cells of hexagonal β- and body-centered α-$ThSi_2$. The light/dark atoms are Si/Th.

confining C_6 hexagons, while the Bloch functions of the C−C antibonding π^* band mostly do, the interlayer and the π^* bands hardly hybridize with each other. However, buckling the graphene layers or shifting the Ca positions parallel to the layers breaks this approximate symmetry and hybridizes the two bands strongly. The resulting electron−phonon coupling causes superconductivity with T_c = 11, 6, and 8 K, in respectively CaC_6, YbC_6, and Ca(AlSi).[12,13]

Despite the recent interest in these heavily electron-doped graphites, very little theoretical work has been performed in studying the origin of superconductivity—and even the bonding—in the six-electron compound β-$ThSi_2$, isostructural with MgB_2. Here, intercalation is in *all* of the hexagonal holes. In the present paper, we shall investigate—not only for β-$ThSi_2$ but also for the "twisted" allotrope α-$ThSi_2$—whether interlayer and π^* bands are present at the Fermi level, and we shall also study the bonding.

$ThSi_2$ is dimorphic and can exist in one of two structures depending upon the temperature of preparation.[15,16] The hexagonal, planar form, β-$ThSi_2$, shown at the top of Figure 1, has the same AlB_2 structure as MgB_2: the silicon sublattice is cubic graphite (honeycomb), and the thorium atoms are between two parallel hexagons, thus forming triangular layers. The tetragonal form, α-$ThSi_2$, is a *twisted* version of this and is shown at the bottom of Figure 1: starting out from a σ bond in the z direction (Si_1−Si_2 or Si_3−Si_4), the two remaining sp^2 directed orbitals at one end of the bond (Si_1 or Si_3) form σ bonds lying in the xz plane, while those at the other end (Si_2 or Si_4) are *rotated* by 90° to form σ bonds lying in the yz plane. The silicon hexagons are thus cut and twisted to form intersecting stacks of Si_5 platelets running in the y and x directions. At the intersections are the thorium atoms, which have 12 nearest silicon neighbors like in β-$ThSi_2$ but are confined by a pair of Si_5 platelets both in the x direction and in the y direction. Note that the meaning of x and y for the α form corresponds to z for the β form. β-$ThSi_2$ has one and α-$ThSi_2$ has two formula units per primitive cell. Finally, we remark that the thorium sublattice of α-$ThSi_2$ is that of a high-pressure form of elemental cesium (Cs−IV).[17,18]

X-ray photoemission spectroscopy (XPS) has been performed on α-$ThSi_2$.[19] The Fermi level was shown to have predominantly thorium 6d character. A peak appearing at ∼−2.5 eV was attributed to thorium 6d and silicon 3p bonding states, whereas a peak located at ∼−6 eV was found to be a mixture of silicon 3s and 3p. Finally, at ∼−8 eV, a peak corresponding to almost pure silicon 3s was found. The results were also thought to indicate charge transfer from thorium to silicon. To the best of our knowledge, there have not been any XPS studies on β-$ThSi_2$.

$ThSi_2$ is superconducting with a relatively low T_c = 2 and 3 K for the β and α forms, respectively.[20] Substitution of silicon by iridium;[19,21] rhodium;[21] and cobalt, nickel, and platinum[22] has led to the preparation of other superconducting materials. For $ThRh_xSi_{2-x}$ and $ThIr_xSi_{2-x}$ in the α-$ThSi_2$ structure, the lattice parameter c decreased when $x > 0.75$, due to the formation of Rh−Rh or Ir−Ir bonds.[21] The decrease in c also resulted in an increase of T_c up to ∼6.5 K for $ThRh_{0.96}Si_{1.04}$ and ThIrSi. It was postulated that the increase in T_c may be a result of an increase in the density of states at the Fermi level due to the formation of metal−metal bonds, or due to the decrease of c.

Previous band-structure work has focused on understanding the relative structural stability of the β-and α-Si_2 sublattices as a function of electron doping into the π^* band, that is, beyond four electrons per Si.[23] For this purpose, the extended Hückel method was used, and an interlayer band was not considered. Whereas, in the planar structure, each Si $p_\perp$ orbital interacts (ppπ) with its three nearest neighbors, it only interacts with two of them in the twisted structure, because the third $p_\perp$ orbital is rotated 90° away. As a result, the π band is more narrow in the twisted structure, which should therefore be more stable than the planar structure once the doping is into the upper, antibonding half of the π band, the π^* band.[23]

In the present paper, we first of all investigate whether there is an interlayer and a π^* band at the Fermi level in planar $ThSi_2$, that is, not only at fillings 4.3−4.5 but at a filling as high as six electrons per Si, and, hence, whether the superconductivity observed in β-$ThSi_2$ below 2 K could have the same cause as in CaC_6, YbC_6, and Ca(AlSi).

Next, we pose the same question for the twisted allotrope observed to be superconducting below 3 K. Since in this case there are no Si layers, but only Si_5 platelets, it is not so obvious that an "interlayer" band exists, and even if it did, it is not so obvious that only when the platelets buckle or when Th is displaced in the z direction would the "interlayer" band hybridize with the π^* band. Apart from this, the k-space band structure of α-$ThSi_2$ is bewilderingly complicated due to the many types of bands, the cell doubling, and the local rotations.

We shall therefore attempt to describe the electronic structure *in real space*. To do this, we seek *minimal* sets of atom-centered, localized orbitals which *completely* span the DFT band structure in a certain energy region and then show

(15) Jacobson, E. L.; Freeman, R. D.; Tharp, A. G.; Searcy, A. W. *J. Am. Chem. Soc.* **1956**, *78*, 4850–4852.
(16) Brown, A. *Acta Crystallogr.* **1961**, *14*, 860–865.
(17) Takemura, K.; Minomura, S.; Shimomura, O. *Phys. Rev. Lett.* **1982**, *49*, 1772.
(18) von Schnering, H. G.; Nesper, R. *Angew. Chem., Int. Ed. Engl.* **1987**, *26*, 1059.
(19) Chevalier, B.; Zhong, W. X.; Buffat, B.; Etourneau, J.; Hagenmuller, P.; Lejay, P.; Porte, L.; Duc, T. M.; Besnus, M. J.; Kappler, J. P. *Mater. Res. Bull.* **1986**, *21*, 183–194.
(20) Hardy, G. F.; Hulm, J. K. *Phys. Rev.* **1954**, *93*, 1004–1016.
(21) Lejay, P.; Chevalier, B.; Etourneau, J.; Tarascon, J. M.; Hagenmuller, P. *Mater. Res. Bull.* **1983**, *18*, 67–71.
(22) Zhong, W. X.; Ng, W. L.; Chevalier, B.; Etourneau, J.; Hagenmuller, P. *Mater. Res. Bull.* **1985**, *20*, 1229–1238.
(23) Zheng, C.; Hoffmann, R. *Inorg. Chem.* **1989**, *28*, 1074–1080.

pictures of these orbitals together with the band structure decorated by the various orbital characters, the so-called *fat bands*. For instance, can the set containing the Si s, the three Si p, and the Th s orbitals, that is, the {2Si s, p_x, p_y, p_z, Th s} set with nine orbitals per $ThSi_2$, describe the occupied bands perfectly, and the lowest unoccupied bands approximately, provided that the orbitals are allowed to take shape after the structure? The table of contents graphic shows that the Th s orbital obtained for the planar allotrope is shaped as a torus, like the interlayer Wannier function in the intercalated graphites, while for the twisted allotrope it is simply a *twisted torus!* For both allotropes, the band structure decorated with this Th s character does identify an interlayer band (two bands for the α-allotrope), but this band is cut not only by π^* bands, with which it hardly hybridizes, but also by σ^* bands, with which it hybridizes weakly so that avoided crossings occur. Our Th s orbital is therefore *not* a Wannier function which can be projected out of the band structure by the usual means,[24−26] but it is a member of a minimal, local-orbital basis set, which is complete for the relevant group of bands. Had this group of bands been isolated from—or not been hybridizing with—other bands, this set *would* be a set of generalized Wannier functions, if ortho-normalized. We shall therefore refer to, for example, our Th s function as being Wannier-*like* or, more simply, a Wannier *orbital*.

Our orbitals are the newly developed muffin-tin orbitals of order *N*, *N*MTOs,[27−30] and this paper has the dual purpose of demonstrating their use. The meaning of *N* is that a set of *N*MTOs spans those solutions of the one-electron Schrödinger (Dirac, Kohn−Sham, etc.) equation whose energies coincide with a chosen set of $N + 1$ energies, $\epsilon_\nu(\nu = 0, N)$, *exactly*, and provides a solution with energy ε_i to within an error proportional to $(\varepsilon_i - \epsilon_0)(\varepsilon_i - \epsilon_1)...(\varepsilon_i - \epsilon_N)$. This may be called *N*th-order polynomial approximation for the Hilbert space of Schrödinger solutions. The *N*MTO set converges to a complete set as the mesh becomes denser and denser ($N \rightarrow \infty$), provided that this set of bands is isolated from all other bands. The *N*MTO set is constructed *directly*, in real space for example from the scattering solutions for the mesh energies, ϵ_ν, and for an *overlapping* muffin-tin approximation (OMTA), $\Sigma_R v_R(|\mathbf{r} - \mathbf{R}|)$, to the self-consistent one-electron potential,[31] that is, from the regular partial waves, $\phi_{Rl}(\epsilon_\nu, |\mathbf{r}-\mathbf{R}|)\, Y_{lm}(\widehat{\mathbf{r}-\mathbf{R}})$, and localized solutions, $\psi_{Rlm}(\epsilon_\nu, \mathbf{r} - \mathbf{R})$, of the wave equation in the interstitial. An individual *N*MTO, $\chi_{Rlm}(\mathbf{r} - \mathbf{R})$ centered at site *R* and with formal angular-momentum *lm* around that site, is a solution (in the polynomial approximation) of Schrödinger's equation for the solid (in the OMTA) with the boundary condition that the projection of $\chi_{Rlm}(\mathbf{r} - \mathbf{R})$ onto $\delta(|\mathbf{r}-\mathbf{R}'|_{a'})\, Y_{l'm'}(\widehat{\mathbf{r}-\mathbf{R}'})$, with a' being some hard-core radius, *vanishes* for *all* $R'l'm'$ in the *N*MTO set, except the *Rlm*. As an example, the Th s *N*MTO of the {2Si s, p_x, p_y, p_z, Th s} set may have Th s character on its own site, but *none* on any *other* Th site, and *neither s nor any p* character on any Si site. This hard-core boundary condition is what *localizes* the orbital. The information the orbital provides comes from the remaining characters, those for which there are no orbitals in the set, for example the Th p, d, etc, and the Si d etc. characters, as well as from the interstitial shape, because those parts are determined by the requirement that the orbital be an eigenfunction of Schrödinger's equation for the solid. Those remaining characters give the structural dependence, for example the difference between the Th s orbital in the planar and the one in the twisted structure. Technically speaking, those remaining characters are folded down into the orbitals by Löwdin partitioning.

Compared with the maximally localized Wannier functions of Marzari and Vanderbilt, *N*MTOs are atom-centered *orbitals* rather than general functions, and they are localized by the above-mentioned hard-core boundary conditions, rather than by minimizing their spread $\langle r^2 \rangle$. *N*MTOs are not projected out from the large set of Bloch functions but are generated directly from the partial-wave solutions for an overlapping MT potential. As a consequence, they may be generated in real space and do not require translational symmetry. *N*MTO sets are not orthonormal (but may of course be Löwdin orthonormalized) and, as a consequence, could be more localized than orthonormal Wannier functions. For a given crystal, both sets are in principle complete and could therefore be transformed into each other. *N*MTOs are, however, more similar in spirit to a recently proposed set of localized orbitals used to span either the occupied or the virtual Hilbert spaces and generated directly from atomic orbitals using a least-change strategy.[32]

After having used the {2Si s, p_x, p_y, p_z, Th s} set of *N*MTOs to find the interlayer band and to identify the Si σ and π bands, we shall try to use the *N*MTO machinery to investigate the *bonding*, in the sense that we seek a basis set which spans *only* the *occupied* bands. This means that a set contains exactly *as many orbitals as there are electron pairs* and *spans the occupied bands*. With such a *truly minimal* set, the band-structure energy is simply the sum of the energies of the orthonormalized orbitals; that is, to compute the sum of the occupied one-electron states, we need not integrate over the Brillouin zone but merely sum over the energies of the few different orbitals in the set. Truly minimal sets of localized orbitals exist for insulators, but not for metals, unless symmetry breaking and a long range are allowed.[29] A simple example of insulators are sp^3-bonded AB semiconductors, where it was found[33] that putting the four s and p *N*MTOs on the anions, but none on the cations, that is, starting from a completely ionic description, gives an exact valence band whose anion-centered sp^3-symmetrized *N*MTOs are so spread out that they become, in fact, the well-known bond orbitals. This worked even for diamond-structured Si, even with the orbitals placed on the cations. This means that one

(24) Satpathy, S.; Pawlowska, Z. *Phys. Status Solidi* **1988**, *145*, 555.
(25) Marzari, N.; Vanderbilt, D. *Phys. Rev. B.* **1997**, *56*, 12847.
(26) Ku, W.; Rosner, H.; Pickett, W. E.; Scalettar, R. T. *Phys. Rev. Lett.* **2002**, *89*, 167204.
(27) Andersen, O. K.; Saha-Dasgupta, T. *Phys. Rev. B.* **2000**, *62*, R16219.
(28) Andersen, O. K.; Saha-Dasgupta, T.; Tank, R. W.; Arcangeli, C.; Jepsen, O.; Krier, G. Developing the MTO Formalism. In *Electronic Structure and Physical Properties of Solids. The Uses of the LMTO Method.*; Dreyssé, H., Ed.; Springer Lecture Notes in Physics: Berlin, 2000.
(29) Zurek, E.; Jepsen, O.; Andersen, O. K. *ChemPhysChem* **2005**, *6*, 1934–1942.
(30) Zurek, E.; Autschbach, J.; Andersen, O. K. Downfolding and N-ization of Basis Sets of Slater Type Orbitals. In *Computation in Modern Science and Engineering, Proceedings of the International Conference on Computational Methods in Science and Engineering 2007*; Simos, T. E., Maroulis, G., Eds.; American Institute of Physics: College Park, MD, 2007; Vol. *2*, part B, pp 1421−1424.
(31) Zwierzycki, M.; Andersen, O. K. *Acta Phys. Pol., A* **2009**, *115*, 64–68.
(32) Ziolkowski, M.; Jansik, B.; Jorgensen, P.; Olsen, J. *J. Chem. Phys.* **2009**, *131*, 124112.
(33) Andersen, O. K.; Saha-Dasgupta, T.; Ezhov, S. *Bull. Mater. Sci.* **2003**, *26*, 19–26.

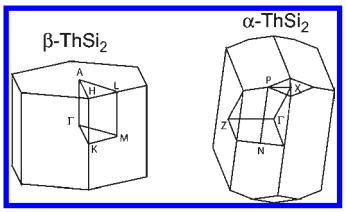

Figure 2. The Brillouin zones (BZ) of hexagonal β-$ThSi_2$ (left) and body-centered tetragonal α-$ThSi_2$ (right). The orientations are like in Figure 1. Going from Γ in the x or y direction in the α-$ThSi_2$ BZ, one reaches a Z point at the common face center of two neighboring zones.

can think of each (spin-polarized) *N*MTO as an electron which, despite using ionic labeling, develops the correct covalent character through the downfolding. The same was found for the sp^2 σ bands in graphites.[29] Their half-filled π band is a simple example of a metal. Here, we found that the occupied part is described exactly by an *N*MTO set with *one* p_z *N*MTO on every *second* C. This orbital spreads out toward its three neighbors, which carry no p_z orbital. In this case, the symmetry cannot be restored by forming other linear combinations, because this may at most generate bond orbitals between every second carbon pair; the symmetric answer is a *resonating* bond. Nevertheless, the bond energy of graphite *is* the energy of the spread-out p_z *N*MTO on every seond C, plus that of the three σ bonds.

α- and β-$ThSi_2$ are metals with a real Fermi surface, not just a Dirac point like graphite, and it would be a complicated matter to find a set of orbitals which exactly spans the occupied—and none of the unoccupied—bands; it would, for example, require a basis set which completely breaks the translational symmetry. We shall, nevertheless, try to learn about the part of the *bonding* which is not related to Fermi surface effects by keeping the translational symmetry and picking various basis sets with three orbitals (six electrons) per Si, that is, by deleting three of the orbitals in the nine-orbital {2Si s, p_x, p_y, p_z, Th s} set and seeing which six-orbital/$ThSi_2$ set best reproduces the occupied bands.

Before using minimal *N*MTO representations, we shall calculate the DFT band structures with the standard linear muffin-tin orbital method (TB-LMTO) and discuss them in terms of the relatively large basis of orthonormal LMTOs.[34,35] Moreover, in order to understand the influence of thorium, we shall also calculate the band structures of the β and α Si_2 sublattices without thorium.

2. Computational Details

Structure of β-$ThSi_2$. The β-$ThSi_2$ structure is hexagonal and has the space group $P6/mmm$ (191) with thorium and silicon located in the 1a and 2d Wyckoff positions. Its primitive cell contains one formula unit and has dimensions $\sqrt{3}a/2 \times a \times c$. The lattice parameters a and c were obtained from experimental data[15] as being 3.985 and 4.220 Å, respectively. The primitive translation vectors, expressed in Cartesian coordinates, are $\mathbf{T_1} = (a, 0, 0)$, $\mathbf{T_2} = (-a/2, \sqrt{3}a/2, 0)$, $\mathbf{T_3} = (0, 0, c)$. The primitive reciprocal lattice vectors are $\mathbf{G_1} = (2\pi/a, 2\pi/\sqrt{3}a, 0)$, $\mathbf{G_2} = (0, 4\pi/\sqrt{3}a, 0)$, and $\mathbf{G_3} = (0, 0, 2\pi/c)$. Figure 2 shows the Brillouin zone (BZ; primitive cell of the reciprocal lattice) with the high symmetry points: $\Gamma = (0, 0, 0)$, $A = (\mathbf{G_3}/2) = (0, 0, \pi/c)$, $M = (\mathbf{G_2}/2) = (0, 2\pi/\sqrt{3}a, 0)$, $L = (\mathbf{G_2} + \mathbf{G_3})/2 = (0, 2\pi/\sqrt{3}a, \pi/c)$, $K = (\mathbf{G_1} + \mathbf{G_2})/3 = (2\pi/3a, 2\pi/\sqrt{3}a, 0)$, and $H = (2\mathbf{G_1} + 2\mathbf{G_2} + 3\mathbf{G_3})/6 = (2\pi/3a, 2\pi/\sqrt{3}a, \pi/c)$.

Structure of α-$ThSi_2$. α-$ThSi_2$ is body-centered tetragonal and has the space group $I4_1/amd$ (141), with the thorium and silicon atoms located in the 4a and 8e Wyckoff positions, respectively. The primitive cell contains two formula units and has the dimensions $a \times a \times c/2$. The lattice parameters a and c were taken from experimental data as being respectively 4.126 and 14.346 Å.[36] In Cartesian coordinates, the primitive translation vectors are $\mathbf{T}_1 = (a, 0, 0)$, $\mathbf{T}_2 = (0, a, 0)$, and $\mathbf{T}_3 = (a/2, a/2, c/2)$. The primitive reciprocal lattice vectors are $\mathbf{G}_1 = (2\pi/a, 0, 2\pi/c)$, $\mathbf{G}_2 = (0, 2\pi/a, 2\pi/c)$, and $\mathbf{G}_3 = (0, 0, 4\pi/c)$. Figure 2 shows the Brillouin zone with the high symmetry points: $\Gamma = (0, 0, 0)$, $Z = (\mathbf{G}_3/2) = (0, 0, 2\pi/c)$, $N = (\mathbf{G}_1/2) = (\pi/a, 0, \pi/c)$, $P = (2\mathbf{G}_1 + 2\mathbf{G}_2 - \mathbf{G}_3)/4 = (\pi/a, \pi/a, \pi/c)$, and $X = (\mathbf{G}_1 + \mathbf{G}_2 - \mathbf{G}_3)/2 = (\pi/a, \pi/a, 0)$.

Density-Functional Calculations. The Vosko−Wilk−Nusair[37] local exchange correlation potential was used along with the Perdew−Wang[38] generalized gradient approximation. Scalar relativistic effects were included. It was not necessary to take spin−orbit coupling into account, since it was found to have a negligible effect on the band structure and the Fermi surface of both allotropes.

The charge self-consistent calculations were performed with the Stuttgart LMTO code[39] and a nearly orthonormal basis set which includes the Si s, p, and d LMTOs and the Th s and d LMTOs, with the Th p and f partial waves downfolded. Explicit inclusion of Th f LMTOs in the basis had a negligible effect. The atomic-sphere radii employed were $s_{Si} = 1.254$ and $s_{Th} = 2.148$ Å for β-$ThSi_2$ and $s_{Si} = 1.310$ and $s_{Th} = 2.160$ Å for α-$ThSi_2$. In neither case was it found necessary to insert empty interstitial spheres. In the calculations for the Si_2 sublattices alone, Th was of course substituted by an empty sphere of the same size, so the formula unit is ESi_2. The self-consistent calculations utilized 980/961 irreducible k points in the tetrahedron integrations.[40] In order to clearly resolve the van Hove singularities, 3501/3101 irreducible k points were used to generate the density of states for β-$ThSi_2$ and α-$ThSi_2$, respectively.

Our present version of the *N*MTO program[33] is not self-consistent, so as input we used the self-consistent ASA potential generated by the LMTO code as described above. The choice of hard-core radii is not crucial as long as the hard spheres do not overlap. We used $a_{Si} = 1.20$ and $a_{Th} = 1.37$ Å, which are roughly 85% of the tabulated atomic radii. The downfoldings and energy meshes employed for particular calculations will be given below.

In all band structures shown in this paper, the zero of enegy is the Fermi level and the fatness of a band is proportional to a projection onto a particular *orthonormal* basis of LMTOs or *N*MTOs. Hybridization in such fat band structures shows up as shared characters.

Projection onto orthonormal LMTOs is identical with projection onto partial waves truncated outside—and normalized inside the atomic s spheres.[35]

The *N*MTOs shown in this paper as $|\chi| = \text{const}$ − contours, with red and blue indicating the sign of χ, are prior to symmetric (Löwdin) orthonogonalization.

3. Electronic Structure of β-$ThSi_2$

3.1. Description in Terms of the Large LMTO Set. 3.1.1. β-Si_2 Sublattice. Before considering the band structure of β-$ThSi_2$, let us start by considering the band structure of the Si_2 *sublattice*, that of hexagonal,

(34) Andersen, O. K. *Phys. Rev. B.* **1975**, *12*, 3060.
(35) Andersen, O. K.; Jepsen, O. *Phys. Rev. Lett.* **1984**, *53*, 2571.
(36) Brauer, G.; Mitius, A. *Z. Anorg. Allg. Chem.* **1942**, *249*, 325–339.
(37) Vosko, S. H.; Wilk, L.; Nusair, M. *Can. J. Phys.* **1980**, *58*, 1200.
(38) Perdew, J. P.; Wang, Y. *Phys. Rev. B* **1986**, *33*, 8800.
(39) The Stuttgart TB-LMTO-ASA code, version 4.7. See http://www.fkf.mpg.de/andersen/ (accessed Dec 2009).
(40) Blöchl, P. E.; Jepsen, O.; Andersen, O. K. *Phys. Rev. B* **1994**, *49*, 16223.

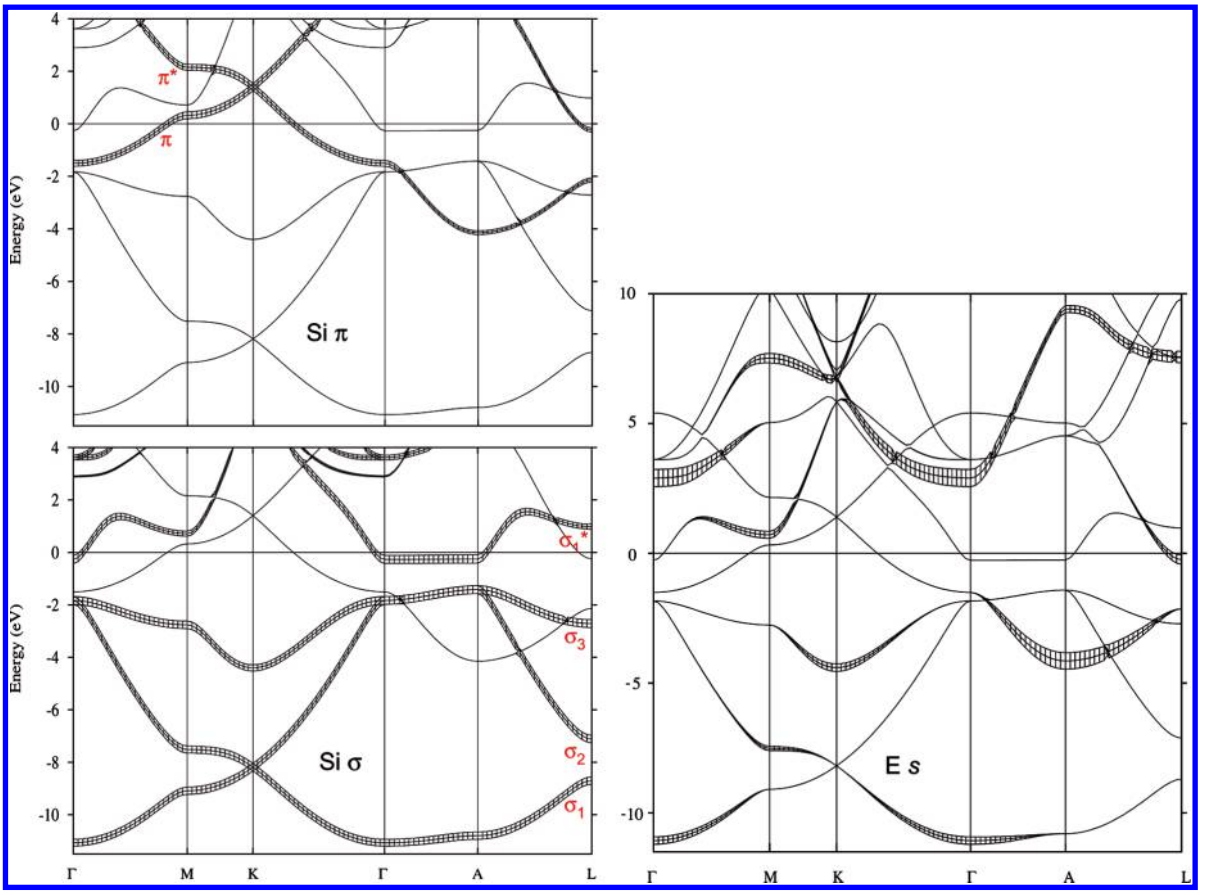

Figure 3. Energy bands for the four-electron/Si sublattice, β-ESi_2, decorated with orthonormal LMTO characters (fat bands). The Fermi energy is zero.

graphite-structured ESi_2 with the lattice constants of $ThSi_2$. This band structure is shown in Figure 3, where the three panels are decorated with, respectively, the sum of the Si s, p_x, and p_y characters, which is the same as the sum of the three Si sp^2 characters, the Si p_z character, and E s characters. These characters refer to projections on orthonormal LMTOs, which are the same as those onto partial waves truncated outside and normalized inside the atomic spheres (see the Computational Details).

The sp^2 in-layer bonding/antibonding (σ/σ^*) bands and the p_z in-layer bonding/antibonding (π/π^*) bands are seen to cross without hybridizing with each other. This is because the sp^2 orbitals are even and the p_z orbitals are odd with respect to the Si layer. They can therefore only interact if they are on neighboring layers, and if their Bloch sums have $k_z \neq 0$ and $\neq \pi/c$. In those cases, the hybridization is very weak.[41]

We see that the Fermi level (zero of energy) for four electrons/Si is *not* at the Dirac point at K where the π and π^* bands stick together, as is the case for graphite, C_2,[29] because the bottom of the σ^* band (along ΓA) falls *below* this energy. In fact, the bottom of the lowest σ^* band, σ_1^*, along ΓA ($k_x = 0$, $k_y = 0$) is the singly degenerate, antibonding s state, whereas in C_2, it is the doubly degenerate, antibonding (p_x, p_y) state, which in Si_2 is seen to lie 4 eV above the antibonding s state. The reason is that in silicon the 4s level is further below the 3p level than is 3s relative to 2p in carbon.[42] For that reason, the strength of the σ bond in Si_2 is only about half that in C_2, and this longer bond is what causes the width of the Si_2 π/π^* band to be only half of that in graphite. We emphasize that the Si−Si bond (of length $a/\sqrt{3} = 2.30$ Å) is not being stretched by Th, because in pure, hexagonal Si_2 at 16 GPa where the inter-layer distance is compressed, this bond is even longer (2.55 Å). This means that, in $ThSi_2$, thorium helps binding the Si_2 sublattice together. Finally, we remark that also the calculated band structure of EAlSi[12] exhibits a low-lying, singly degenerate σ^* band.

The decoration with E s character identifies the interlayer band in Si_2. Near the Γ point, this band—not spanned by any Si orbital—is 3 eV above the Fermi level and lies above the σ_1^* and π bands. Having orbitals which are even with respect to the midplane between two Si layers, the interlayer band cannot hybridize with the p_z bands when $k_z = 0$, but only when $k_z = \pi/c$, and not with the sp^2 bands when $k_z = \pi/c$, but only when $k_z = 0$. Due to the different directions of the p_z and sp^2 orbitals, the hybridization with the interlayer band is stronger for the former, when allowed. Since the orbitals for the interlayer band are invariant to the 6-fold rotations which take a Si_6 hexagon into itself, the interlayer band hybridizes less with the antibonding σ^* and π^* bands, whose Bloch waves mostly change sign upon 6-fold rotations, than with their bonding counterparts, for which this is not the case.

(41) Mazin, I. I.; Andersen, O. K.; Jepsen, O.; Dolgov, O. V.; Kortus, J.; Golubov, A. A.; Kuz'menko, A. B.; van der Marel, D. *Phys. Rev. Lett.* **2002**, *89*, 107002.

(42) *Electronic Structure and the Properties of Solids: The Physics of the Chemical Bond*; Harrison, W. A., Ed.; W. H. Freeman and Co.: New York, 1980.

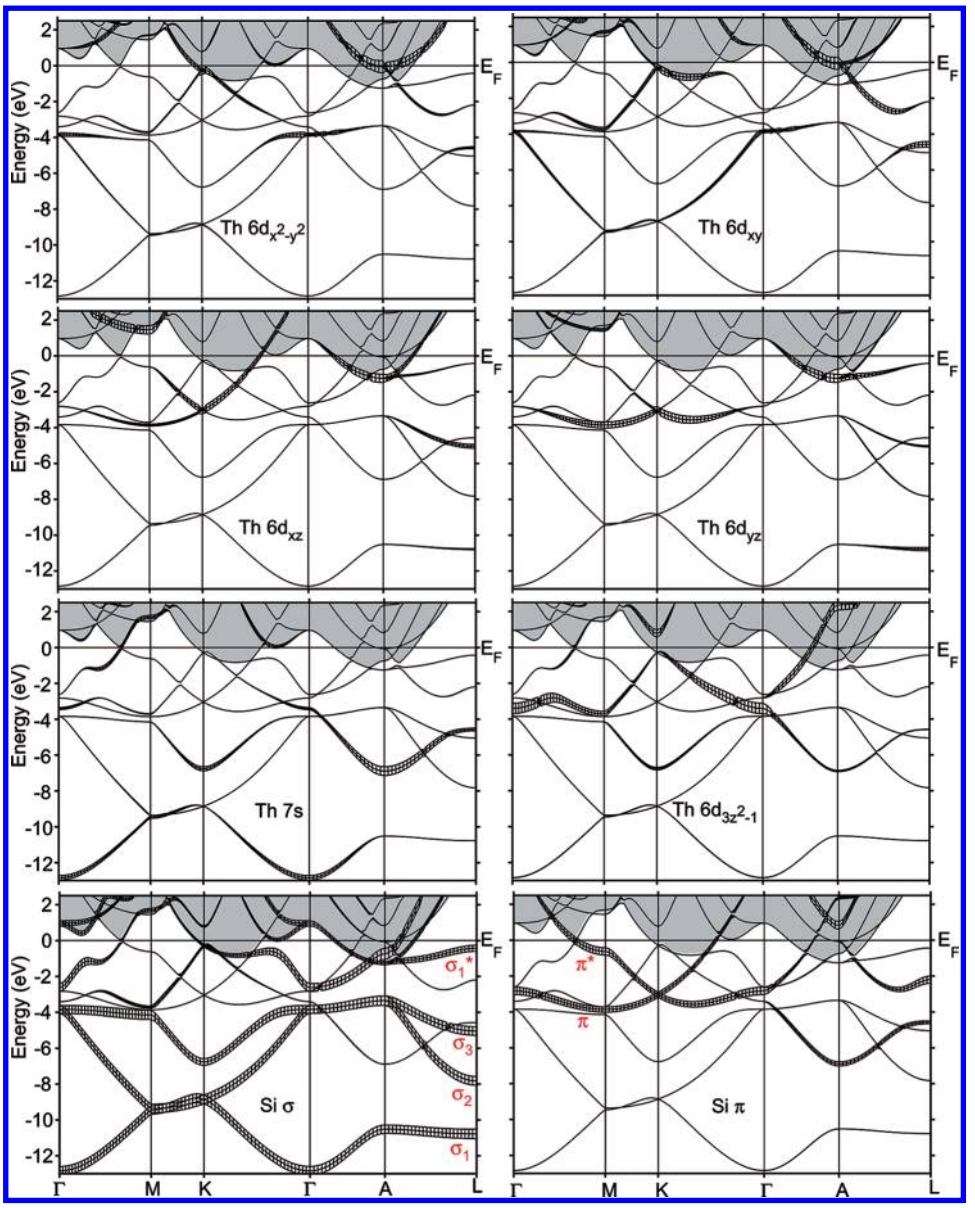

Figure 4. Energy bands of β-$ThSi_2$ with orthogonal LMTO characters (fat bands). At each k point, the area above the 7th band is shaded.

This can all be seen in the figure: At Γ, the interlayer band hybridizes a bit with the lowest (Si s-like) σ band, but not with any σ^* band, although these are much closer in energy, and not with any p_z band. At A, on the other hand, the interlayer band hybridizes strongly with the π band, but not with the π^* band, and not with any sp^2 band. If we now stay with $k_z = \pi/c$, but go from A to L, the hybridization remains to be with the π orbitals only (the π and π^* characters invert near L). If we stay with $k_z = 0$, and go from Γ to M, which is below L in the BZ, the interlayer band starts to hybridize with the s-like σ^* band, which it would otherwise have crossed near M. Here, the hybridized states are split by as much as 7 eV. This does *not* happen in the graphites because there the s-like σ^* band lies many electronvolts higher and therefore does not cross the interlayer band.[13]

3.1.2. β-$ThSi_2$. The fat bands of real β-$ThSi_2$ with six electrons/Si are shown in Figure 4. The Si σ/σ^* and π/π^* bands are seen to remain reasonably intact, although shifted in energy and somewhat deformed compared with those of ESi_2, and so is the interlayer band, whose character has changed to Th, mainly $6d_{3z^2-1}$. The symmetries of these bands remain as discussed previously for Si_2. The bonding Th 6d-like states (say at Γ) lie nearly as low in energy as the bonding Th 7s-like states (say at A), as is found also in elemental Th. Compared with the case in Si_2 (Figure 3), the bottom of the interlayer band has moved down with respect to the σ band—by as much as 5 eV at Γ, where it is now *below* both the π- and the s-like σ^* band. Going from Γ toward A, the interlayer and π^* bands would thus have crossed, but this crossing is avoided by strong hybridization. The strong hybridization between the interlayer and the π^* band persists throughout the $k_z = \pi/c$ ALH plane, where the upper band, the one with predominant interlayer character, is well above the Fermi level and therefore is of little interest to us. Going from Γ toward M in the $k_z = 0$ plane, the interlayer band starts to disperse upward but then hybridizes with the s-like σ^* band and splits, with the lower part being mostly Th d_{3z^2-1}-like and the upper part mostly Th s-like. At M, the

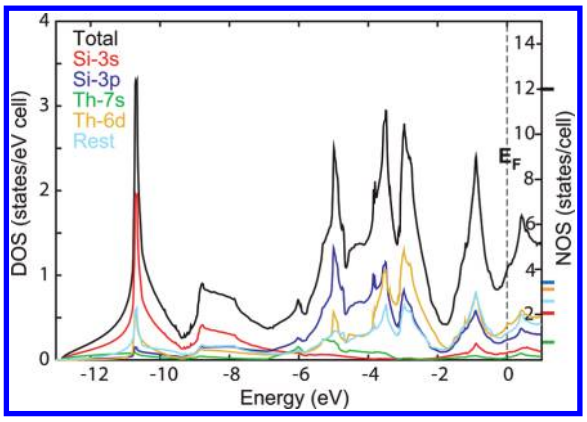

Figure 5. Calculated LMTO-projected and total densities of states for β-$ThSi_2$. The densities of states integrated to the Fermi energy are indicated by ticks on the right-hand axis.

interlayer-σ^* splitting is as large as for ESi_2. Nevertheless, at the Fermi level, the interlayer band (mixed with σ^*) does cross the π^* band without hybridizing with it, like for the superconducting 4.3-electron graphites. Going from Γ toward K, the interlayer band hybridizes increasingly with the bottom of the high-lying Th $d_{x^2-y^2}$ band, which also hybridizes with the second σ^* band, and at the Fermi level, the interlayer band seems to be gapped. This gap persists from K to M.

Going from Γ toward K and onward to M, the lowest σ^* band is pushed down in energy by hybridization with high-lying Th d_{xy} states, and it is this deformed σ^* band which between K and M hybridizes strongly with the interlayer band.

Finally, the π/π^* band around its Dirac point at K has been pushed down in energy by hybridization with high-lying Th $d_{xz/yz}$ states.

With six electrons per Si (Th^{4+} $2Si^{2-}$), $ThSi_2$ has two further bands filled than ESi_2, and these are mainly the lowest σ^* band plus part of the π^* and interlayer bands. Near the Fermi level, its band structure is not as simple as those of the 4.3-electron graphite superconductors, where there are essentially pure π^* and interlayer bands interacting only via lattice deformations. What makes $ThSi_2$ different from those are (1) the Si σ bond is so weak that the lowest, s-like σ^* band crosses the interlayer band, with which it may hybridize, (2) the Fermi level lies nearly two bands higher, and (3) there are strong Th 6d characters. Calculations including the spin−orbit coupling did not change the bands significantly. In order to somewhat better disentangle the bands by integrating out (downfolding) in particular the Th d orbitals, we shall now use the *N*MTO method.

But before doing that, we show the total and LMTO-projected densities of states for β-$ThSi_2$ in Figure 5. Here, "Rest" labels the sum of the densities of states for Si3d, Th7p, and 5f. At the Fermi level, the value of the total density of states is $N(0) = 0.6$ electron/(eV·Si), which is 0.3 per spin, twice the value for the $4^1/_3$-electron/C graphites[13] and for MgB_2.[6−8]

The tick marks on the frame to the right (Figure 5) indicate densities of states integrated to the Fermi level. Of a total of 6×2 electrons per $ThSi_2$, we see that about 1.1×2 are Si s, 1.7×2 are Si p, 0.8 are Th s, and 3.2 are Th d. These numbers refer not only to orthonormal LMTOs but also to partial waves in the atomic s spheres

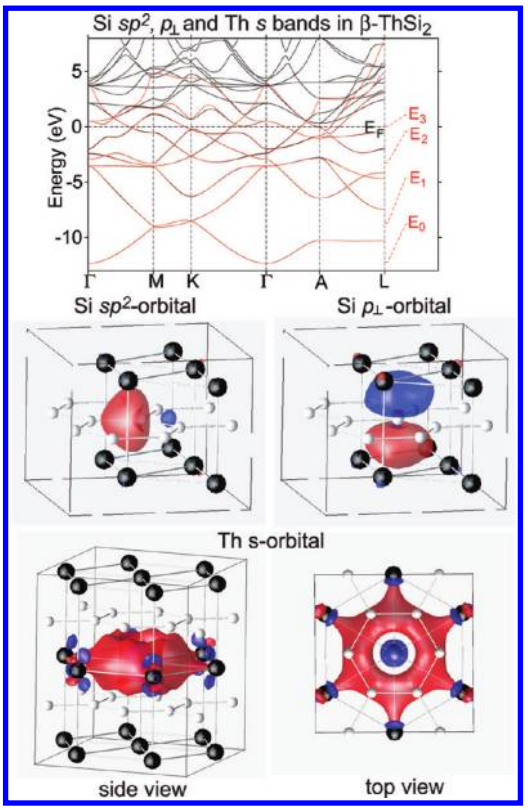

Figure 6. (Top) The band structure of β-$ThSi_2$ calculated with a large *N*MTO basis set {2Si spd, Th sd} in black. In red, the bands calculated with the minimal, nine-orbital {2Si sp, Th s} *N*MTO basis set and the four ($= N + 1$) energy points shown on the right-hand side. (Bottom) The orbitals of the minimal set are shown for the following isosurface values: ±0.10 (Si sp^2), ±0.04 (Si $p_\perp$), and ±0.03 (Th s) in units of the Bohr radius to the power −3/2. For the Th s orbital, we provide views from the side and from the top.

(Computational Details). We shall later compare these densities of states with those for α-$ThSi_2$, for which XPS measurements are available.

3.2. Disentangling the Band Structure with the 9-*N*MTO/$ThSi_2$ Set. In order to decide whether the—somewhat fractured—lowest Th band can be viewed as the ubiquitous interlayer band, which by coupling to the π^* and σ^* bands via Si buckling and Th displacive modes is the likely cause of the observed superconductivity, we extract its Wannier orbital. This we take as the Th s orbital of that complete, minimal *N*MTO basis set,[27−30] which spans the occupied bands and contains also the Si sp^2 and p_z orbitals, that is, a total of nine orbitals/$ThSi_2$. The band structure obtained with this set and a four-point energy mesh ($N = 3$) is shown in red in the upper part of Figure 6. The band structure calculated with a large *N*MTO basis set {2Si spd, Th sd} is given in black for comparison. The two are almost identical on the scale of the figure until slightly above the Fermi level, where for example the Th $d_{x^2-y^2}$ band starts. The black bands are for all purposes exact (and at high energies far more accurate than the LMTO bands shown in Figure 4 and obtained with the energy point for the linear $\varphi-\dot{\varphi}$ expansion taken down at the center of the occupied bands).

The orbitals of the 9-*N*MTO basis are illustrated in the lower part of Figure 6. The Si sp^2 orbitals directed toward the three nearest Si neighbors are the symmetric linear combinations of the Si s, p_x, and p_y *N*MTOs on the same

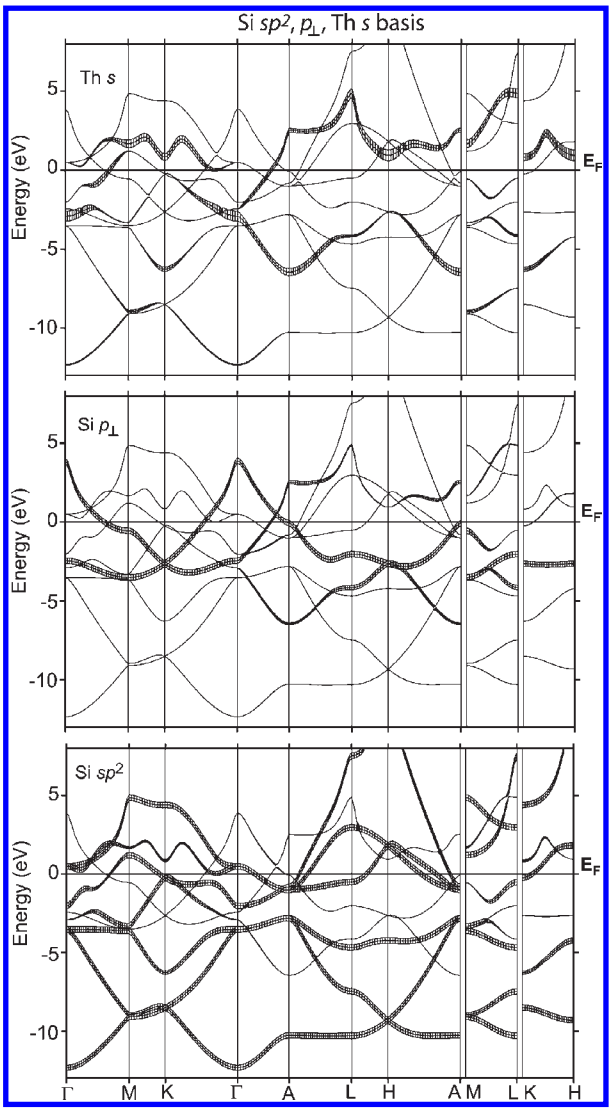

Figure 7. Energy bands of β-$ThSi_2$ along all high-symmetry lines of the BZ and projected onto the orbitals of the minimal 9-*N*MTO basis set (fat bands) in Figure 6.

site, and the Si $p_\perp$ orbital is Si p_z. As explained in the Introduction, the Si p_z *N*MTO, for instance, has no p_z character on any other Si atom in the crystal; no s, p_x, or p_y character on any Si atom, and no Th s character on any Th atom. All other characters are allowed and are determined by the condition that the *N*MTO set span the solutions of Schrödingers equation for the four chosen energies exactly. The Si p_z orbital is similar to the one obtained for graphite in ref 29, except that it contains weak d tails on the three nearest Th neighbors above and three neighbors below (seen better for lower values of the contour).

Of actual interest is the Th s *N*MTO. By construction, it transforms according to the identity representation of the Th point group and is therefore invariant to the 6-fold rotations and the mirror between the Si layers. The downfolding of central d_{3z^2-1} character makes it shaped like a torus with a central hole and a change of sign. Downfolding of all p and d characters on the six Th neighbors makes it spiky. We see that these characters are mainly Th pd hybrids bonding to the torus.

In Figure 7, we show the nine red bands projected onto the nine Löwdin-orthonormalized *N*MTOs, of which there are six Si sp^2 (or σ/σ^*) orbitals, 2 Si $p_\perp$ (or π/π) orbitals, and one Th s (or interlayer) orbital. This representation is seen to *disentangle* the bands well, and this figure, together with the preceding Figure 6 and the corresponding ones for α-$ThSi_2$, are the most important in this paper. Since the symmetries of the orbitals have not been changed by the downfolding, the symmetry analysis of the bands given previously for β-ESi_2 remains true. For completeness, we have now augmented the right-hand side of the figure so that the bands are shown along *all* high-symmetry directions of the BZ (Figure 2). Note that, along the vertical KH line, all bands are doubly degenerate. Note also that, going from K to H, the $\pi-\pi^*$ degenerate Dirac point hardly disperses, although between Γ and A the π^* band disperses by 5 eV, and so do the hybridizing π and interlayer bands.

From the Si sp^2 and Th s projected bands, we see that the Th s band is fractured by avoided crossings with the first and second σ^* bands in—and near—the central ($k_z = 0$) plane and *between* Γ and the MK zone boundary. Further away from the central plane, the interlayer band is *not* fractured because it does not cross any band with which it could hybridize. Hybridization with the very low-lying π band is however substantial.

Since the nine-orbital basis set {2Si sp, Th s} exactly *spans* the occupied bands, *and* its Th s orbital is very similar to the Ca s Wannier orbital for the interlayer band in CaC_6, and also in EC_2,[13,14] we conclude that the lowest Th band in β-$ThSi_2$ *is* the interlayer band. This suggests that the electron−phonon mechanism of superconductivity in β-$ThSi_2$ is similar to the one in the intercalated graphites with only 4.3 electrons/C. Details do however differ.

What is relevant for the electron−phonon interaction is the band structure *at* the Fermi level. The Fermi-level crossing of the interlayer band along—and near—ΓM is intact because the small gaps with the σ_1^* and σ_2^* bands are respectively below and above ε_F. The only remaining gap is around the middle of the ΓK line. Neglecting that gap, the interlayer sheet of the Fermi surface is seen to be a Γ-centered, nearly spherical electron pocket, like in the 4.3-electron graphites,[13] but larger. Like in the graphites, the Fermi surface also has a π^* sheet which is a Γ-centered hole pocket not hybridizing with the interlayer sheet. In β-$ThSi_2$, the interlayer and π^* sheets nearly touch in the central plane, but the π^* sheet is more prolate; that is, it extends closer toward A. Finally, all three σ^* bands cross the Fermi level and give rise to complicated Fermi-surface sheets. Of relevance for the electron−phonon interaction is the gapping of the interlayer sheet caused by the avoided crossing with the second σ^* band near ΓK, because this reduces the phonon-induced interband coupling between the π^* and the interlayer bands.

On the other hand, intraband coupling on the σ^* sheets via optical bond-stretching modes should be strong. This is pretty much like in MgB_2, except that the Fermi-surface sheets involved are those from the doubly degenerate bottom of the σ^* band instead of the top of the doubly degenerate σ band. The total density of states, $N(0)$, has its largest contribution from the σ^* bands and is twice as large as in MgB_2.

But both cations and anions in $ThSi_2$ are more heavy than in CaC_6 and in MgB_2, so the phonon spectrum is different. Needless to say, proper DFT calculations of the

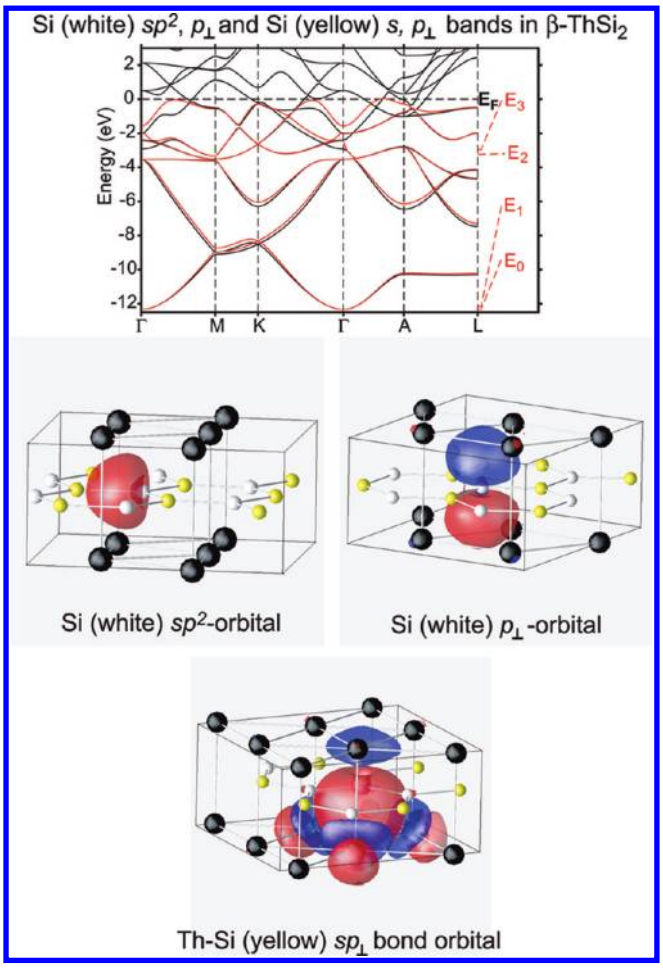

Figure 8. The band structure of β-$ThSi_2$ calculated with a large *N*MTO basis set {2Si spd, Th sd} in black. The red bands have been calculated using a truly minimal six-orbital *N*MTO basis spanning the six lowest bands and an energy mesh with four ($= N + 1$) points. The orbitals are shown at the bottom and are described in the text. The band-structure energy is the sum of the orbital energies. The values of the isosurfaces are ± 0.10 (Si sp^2), ± 0.04 (Si $p_\perp$), and ± 0.02 (Si $sp_\perp$).

phonon spectrum and the electron−phonon interaction should be carried out.

3.3. Describing the Bonding with a 6-*N*MTO/$ThSi_2$ Set. Since the sum of the occupied band energies equals the sum of the energies of the orbitals in a basis which describes *the occupied bands only*, the orbital shapes of such a truly minimal set give real-space information about the bonding. This description is not considered useful for metals, where, in order to reproduce the cutoff at the Fermi energy, the orbitals must have long range and the basis set must have no translational symmetry (unless the Fermi surface coincides with the BZ) so that there are infinitely many different orbitals. However, for a case like $ThSi_2$, it should be possible to obtain a reasonable description of the bonding without invoking the details of the band cutoff. We thus keep the translational symmetry and therefore seek an atom-centered six-orbital basis which reproduces the occupied part of the band structure well.

Hence, we must subtract three orbitals from the complete, nine-orbital set considered above. These three orbitals we find—by trial and error and with the results given in Figure 8—to be the p_x and p_y orbitals on *every second* Si atom (yellow in Figure 8) plus the Th s orbital.

Had we subtracted also the yellow Si s orbital, that is, had every second Si had *no* sp^2 orbitals, the sp^2 orbitals on the remaining Si atoms (white in Figure 8) would have spread onto the empty yellow ones and become sp^2-*bond* orbitals, symmetric with respect to the white and yellow atoms.[29,33] Such a basis would describe the three σ bands, but *no* σ^* band, and yet, we have seen that essentially the lowest, s-like σ^* band is occupied. To include both white and yellow s orbitals therefore makes sense, and the resulting white sp^2 orbital with the p_x and p_y orbitals on the Si neighbors (yellow) downfolded is shown in Figure 8. Its energy is higher (less bonding) than that of the bond-orbital describing only the σ bands.

This white Si sp^2 orbital is allowed to make bonding as well as antibonding linear combinations with the Th−Si sp_z bond orbitals ($sp_\perp$) centered on the yellow Si neighbor toward which it is directed. Such a Th−Si sp_z bond orbital is shown at the bottom of the figure. It is nominally the s minus (or plus) the p_z orbital on a yellow Si atom. Downfolding of *all* Th orbitals has made this sp_z orbital spread out to make bonds with the three Th neighbors toward which it is directed.

Besides the three white sp^2 orbitals and the two yellow sp orbitals bonding with Th, we are left with one white p_z orbital ($p_\perp$) shown in the figure. It bonds only weakly with its six Th neighbors.

We emphasize that the bond energy is 3 times the energy of the white sp^2 orbital, plus twice the energy of the yellow sp_z orbital bonding with Th, plus the energy of the white p_z orbital. Interactions between these orbitals, such as the bonding/antibonding interactions between the white sp^2 and yellow sp_z orbitals, or between the latter and the white p_z orbital merely provide band dispersions whose contributions *cancel* in the total energy.

4. Electronic Structure of α-$ThSi_2$

We now proceed from the planar to the twisted structure (Figure 1). The Si−Si bond is slightly expanded, from 2.30 to 2.38 Å, and the distance between parallel Si platelets is correspondingly contracted, from 4.22 to 4.13 Å. Due to the doubling of the translational cell and the twist invalidating the mirror symmetries globally, the band structures are far more complicated. We shall therefore describe them by comparing them step by step to those of the planar structure. We always use atom-centered orbitals with Si $p_\perp$ perpendicular to the three local bonds, which are the sp^2-directions. For the E *s* and Th *s*-orbitals, directions do not matter. The *k*-space directions are global and chosen as in Figures 1 and 2 with the *x*-direction toward the reader, the *y*-direction up, and the *z*-direction to the left.

4.1. Description in Terms of the Large LMTO Set. 4.1.1. α-Si_2 Sublattice. Here again, we start by considering the band structure of the Si_2 sublattice, that is, of α-ESi_2 with the lattice constants of α-$ThSi_2$.

From the projection onto orthonormal LMTOs in Figure 9, we see that, unlike for the graphite structure and $k_\perp = 0$, hybridization between the sp^2 and $p_\perp$ bands is allowed, but it is very weak. Here, the sp^2 character is the sum of the Si_1 (and Si_3) s, p_x, and p_z and the Si_2 (and Si_4) s, p_y, and p_z characters, while the $p_\perp$ character is the sum of the Si_1 (and Si_3) p_y and the Si_2 (and Si_4) p_x characters.

Like in the planar structure, the top of the σ bands is at Γ, 2 eV below the Fermi level. This coincides with the

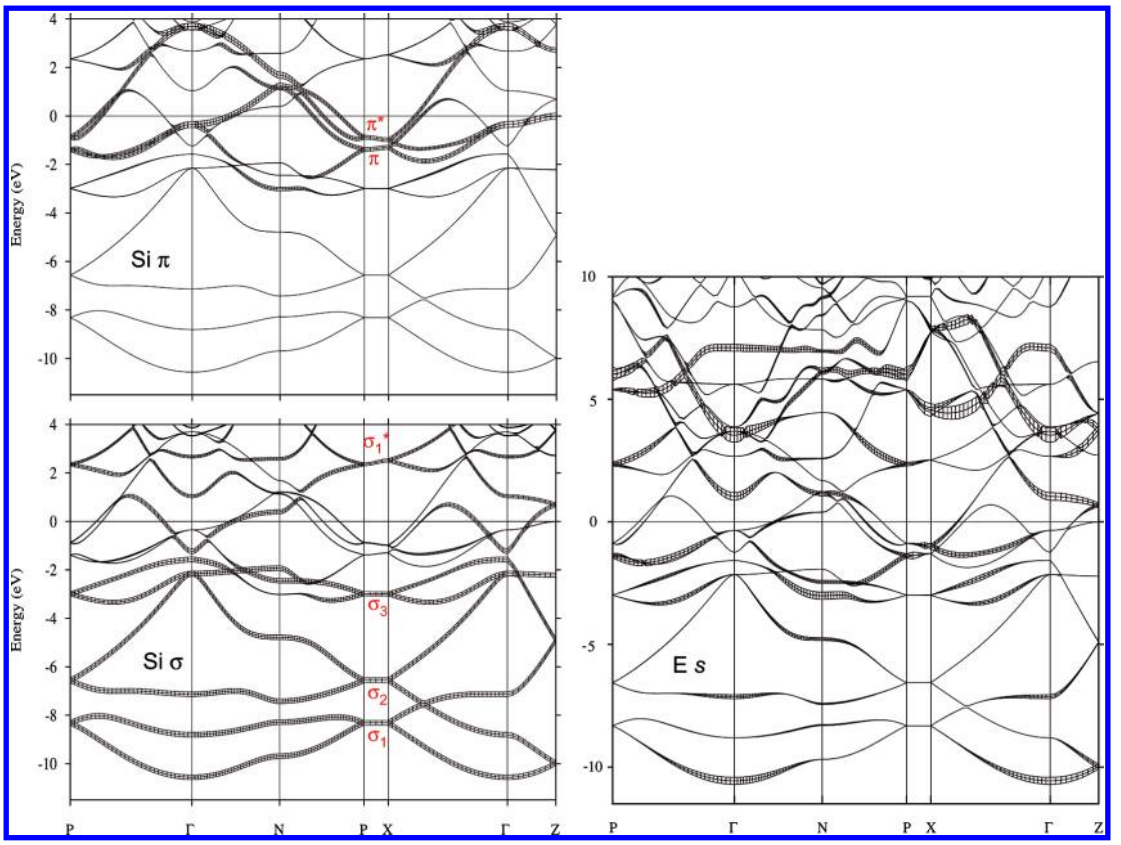

Figure 9. Energy bands for the twisted four-electron/Si sublattice, α-ESi_2, decorated with orthonormal LMTO characters (fat bands). The Fermi energy is zero.

bottom of the two π bands, which at Γ is a bit higher, at −0.5 eV. The bottom of the E s bands is at Γ, 3 eV above the Fermi level, all very much like in the planar structure. The bottom of the σ^* bands lies low also in the twisted structure. Here, the σ and σ^* bands even overlap a bit, and the direct gap between them at Γ is merely 0.4 eV.

The largest difference is that the total width of the four π/π^* bands is merely 6 eV as compared with 9 eV in the planar structure. The reason for this is that one of the three ppπ interactions has been twisted away. This was pointed out in ref 23 and mentioned in the Introduction. Finally, it may be noted that in the twisted structure a band exists connecting the σ and π bands; specifically, the doubly degenerate level at Γ near the top of the σ band and the bottom of the π band at P.

4.1.2. α-$ThSi_2$. For real α-$ThSi_2$, the band structures projected onto othonormal sp^2 and $p_\perp$ LMTOs are shown in Figure 10. The sp^2 bands look similar to those for the planar structure in Figure 4 while the $p_\perp$ bands are more narrow, like for α-ESi_2. Their top is at Γ, merely an electronvolt above the Fermi level for six electrons/Si, because of the twisting away of one of the three ppπ interactions. Also, the influence of Th on the $p_\perp$ bands is strong: one of the four $p_\perp$ bands at −2.5 eV is essentially dispersionless (along the *k* lines included in the figure) since hybridization with high-lying Th d bands suppresses the dispersion of the π^* bands along the Si zigzag chains in the *x* and *y* directions. Around −2 eV, the band structure has a pseudo gap in which, near Γ, there are pure Th $6d_{x^2-y^2}$ states pointing to the centers of the Si_5 platelets. At the Fermi level, well-defined σ^* and π^* bands are seen.

The two interlayer bands having Th 7s character seem very fractionated. To what extent this is real or merely caused by our choice of individual Th d orbitals will be seen in the following section where we integrate out the Th d characters.

The total and projected densities of state for α-$ThSi_2$ in Figure 11 agree well with the experimental XPS data.[19] The region between −12 and −8 eV has primarily Si s character, that between −8 and −5 eV has mostly Si s and p characters, and for that between −5 and 0 eV the major contributions arise from Si p and Th d bands. The positions and characters of the peaks in the XPS data are indicated at the top of the figure. Particularly prominent is the peak caused by the dispersion-less Si $p_\perp$−Th $d_{xz/yz}$ band.

The numbers of LMTO electrons are exactly the same as calculated for the β-$ThSi_2$. The value of the total density of state at the Fermi level is $N(0) = 0.9$ electron/(eV·Si), which is 0.45 per spin and 1.5 times the value in planar β-$ThSi_2$ and 3 times the value for the $4^1/_3$ electron/C graphites and MgB_2.

4.2. Disentangling the Band Structure with the 9-*N*MTO/$ThSi_2$ Set. In complete agreement with the results obtained for β-$ThSi_2$, Figure 12 demonstrates that for α-$ThSi_2$ a minimal basis set consisting of the Si sp^2-, the Si $p_\perp$-, and the Th s-*N*MTOs spans the occupied part of the 18 lowest bands essentially exactly. The Si sp^2 and $p_\perp$ orbitals are as for the planar structure, except that they are turned a bit differently and have more Th character. At first glance, the Th s-*N*MTO shown at the bottom, to the left appears to differ greatly from the interlayer orbital in β-$ThSi_2$, until one realizes that it *is* this torus-shaped

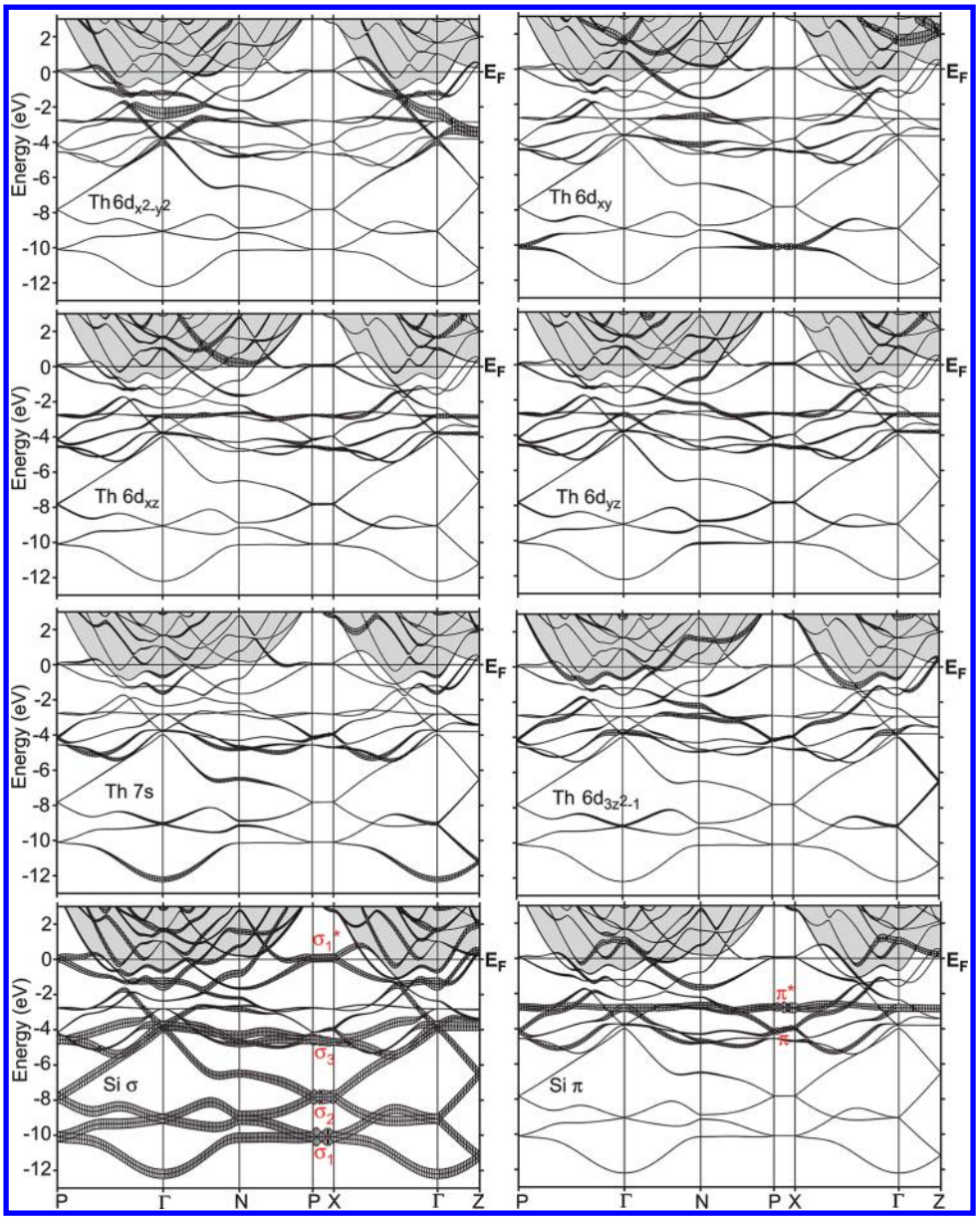

Figure 10. Energy bands of α-$ThSi_2$ with orthogonal LMTO characters (fat bands). At each k point, the area above the 13th band is shaded.

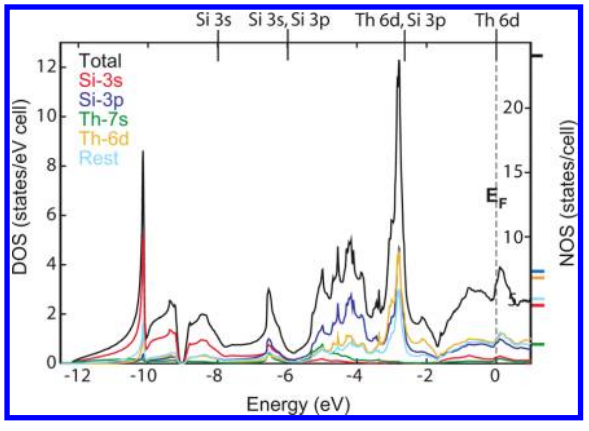

Figure 11. Calculated LMTO projected and total densities of states for α-$ThSi_2$. The densities of states integrated to the Fermi energy are indicated by ticks on the right-hand axis. Ticks at the top frame give the positions and assignments of the peaks in the experimental XPS data of ref 19.

orbital, but cut in two and twisted exactly like the Si sublattice in Figure 1. This is beautiful.

The projection of the 18 red bands onto these *N*MTOs, of which there are 12 Si sp^2 (or σ/σ^*) orbitals, 4 Si $p_\perp$ (or π/π^*) orbitals, and two Th s (or interlayer) orbitals per cell, is shown in Figure 13. For completeness, we have augmented the right-hand side of the figure with the projected band structure along the line from Γ in the k_x or k_y direction to a Z point at the face center between two neighboring Brillouin zones. Along this line, the previously dispersionless $p_\perp$ band does disperse.

This representation largely disentangles the band structure for the twisted allotrope, although by far not so well as for the more symmetric, planar structure. We realize that the Th $d_{x^2-y^2}$ character observed with the large basis set belongs to the tails of the Si sp^2 orbital. This Th $d_{x^2-y^2}$ character peaks where the torus is cut and twisted.

The dispersionless π^* band at −2.5 eV is seen to have neither Th s nor sp^2 character. This means that the origin

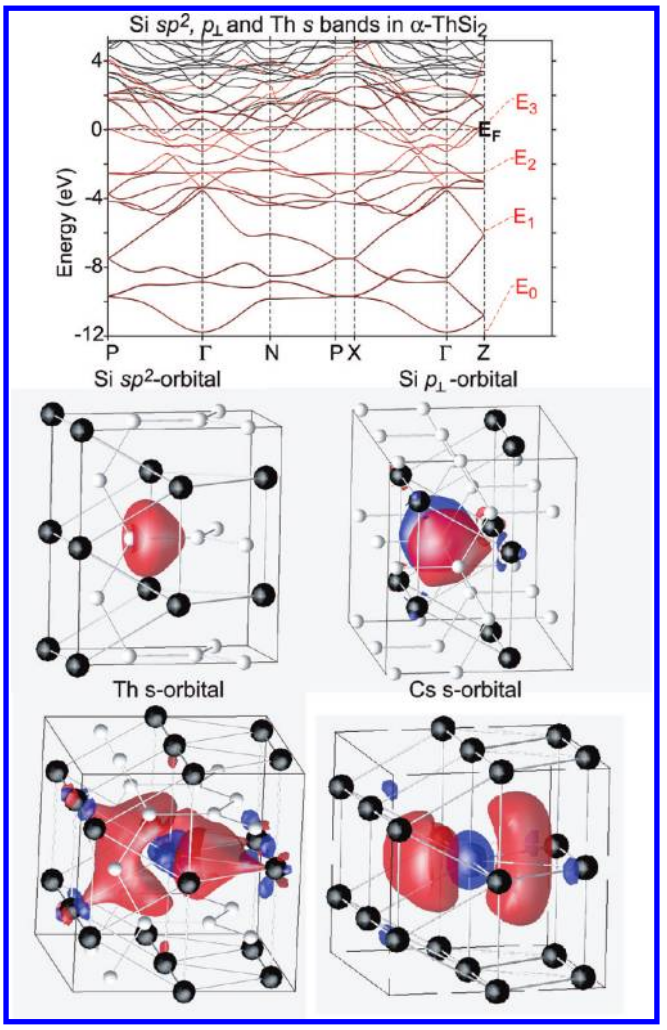

Figure 12. As for Figure 6, but for the twisted α-allotrope. The orbital at the bottom to the right is the Cs s-*N*MTO obtained for the high-pressure Cs−IV phase.[29]

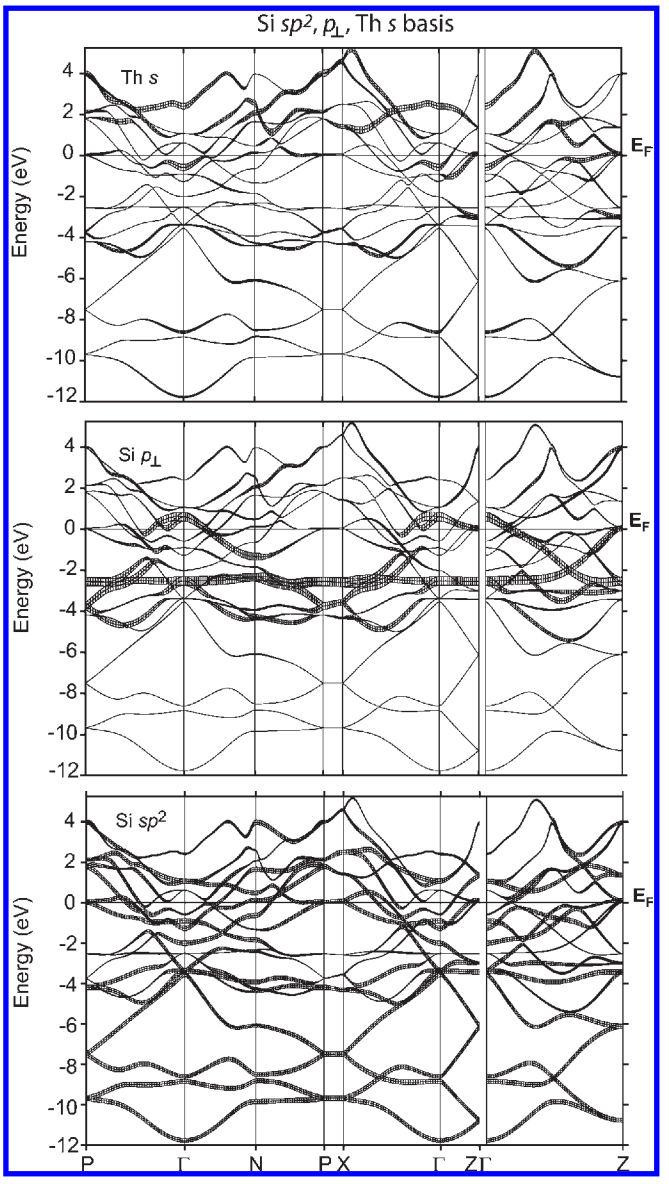

Figure 13. Energy bands of α-$ThSi_2$ with orthogonal *N*MTO characters (fat bands) obtained from the complete minimal basis which spans the 18 lowest bands. The ΓZ line is in the k_x or k_y direction, with *Z* being the common face center of two neighboring Brillouin zones.

of the strong Th d character found in the −2.5 eV peak is from the tail of the Si $p_\perp$ orbital shown in Figure 12. This Th character of the Si $p_\perp$ orbital is bonding and axially symmetric around the Si−Th line. This means that, when placing the same Si $p_\perp$ orbital on the neighboring silicons along the zigzag chain to form a Bloch sum, the bonding Th characters will cancel for the π^* band (but add up for the π band). This is the origin of the Th-induced flatness of the π^* band.

At the Fermi level, the two π^* bands are fairly intact and form small Γ-centered hole surfaces, which are degenerate along k_z and nearly touch the ones from the neighboring zones at Z. This means that they form a string of double pearls along k_z. The lowest interlayer band forms a Γ-centered electron sheet of about the same size. Along the k_x and k_y lines, and possibly along the k_z line, it crosses (one of) the π^* sheets without hybridization, but in other directions it seems to be gapped by hybridization with σ^* bands. The Fermi surface contains several σ^* sheets, and the ones near the PX face of the BZ are doubly degenerate and presumably strongly split by optical bond-stretching modes.

Once again, our findings suggest that the observed superconductivity is caused by electron−phonon interactions of the types known from the 4.3-electron graphites and from MgB_2. In the former, buckling modes of the Si_5 platelets as well as Th *z* modes couple the π^* and interlayer (Th) bands. The total density of states, $N(0)$, is 3 times the values in CaC_6 and MgB_2. Still, the observed values of T_c are considerably lower, so detailed electron−phonon calculations are needed.

4.3. Cs IV. Under pressure, elemental cesium undergoes a number of unusual structural phase transitions.[43] These are believed to be driven by the pressure-induced s → d valence electronic transition.[44] The Cs−IV phase in fact has the same structure as the thorium sublattice in the twisted α-$ThSi_2$.[17] Curiously, band-structure calculations have revealed that the maximum of electron density is along the zigzag region corresponding to the electronegative silicon atoms in α-$ThSi_2$. However, in Cs−IV, there are no atoms on the Si sites. This was first pointed out by

(43) McMahon, M. I.; Nelmes, R. J. *Chem. Soc. Rev.* **2006**, *35*, 943–963.
(44) Sternheimer, R. *Phys. Rev.* **1950**, *78*, 235.

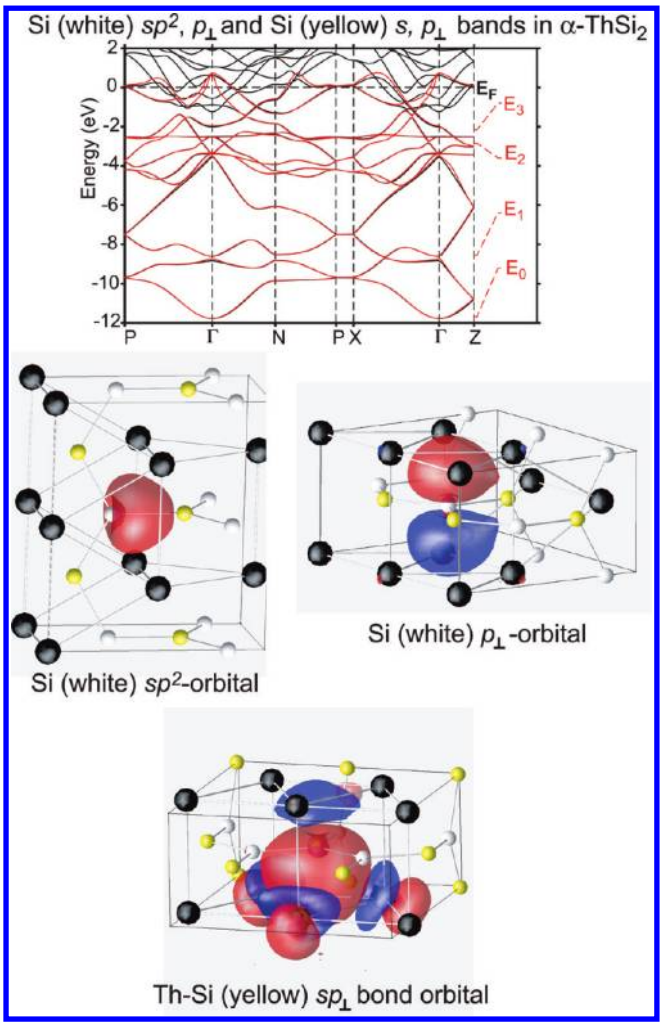

Figure 14. As in Figure 8, but for the 12 lowest bands of the twisted α-structure.

von Schnering and Nesper,[18] who suggested that Cs−IV should therefore be viewed as a cesium electride, Cs^+e^-, where one electron occupies the position of two silicon atoms in α-$ThSi_2$. On the right-hand side of Figure 12, we show the *N*MTO calculated for the Cs−IV conduction band.[29] Clearly, it exhibits a substantial amount of d character and is no longer s-like. Its shape is seen to be that of the Th orbital in α-$ThSi_2$, but turned 90° in order to make up for the lack of a silicon backbone. It suggests that Cs−IV is an electride, with the single electron lying between two planes of cesium atoms.

4.4. Describing the Bonding with the 6-*N*MTO/$ThSi_2$ Set. In complete analogy to the results for β-$ThSi_2$ in Figure 8, we find in Figure 14 that the same truly minimal basis describes the 12 occupied bands reasonably well in the twisted α structure. Thus, the bonding in the two allotropes can be understood in the same manner, but the white Si $p_\perp$ and the yellow $sp_\perp$ orbitals seem to have lower energy in the twisted than in the planar structure due to more bonding with Th.

5. Conclusion

We have used the *N*MTO method for direct generation of minimal basis sets to understand the relation between the electronic structures of graphite-structured silicon, ESi_2, which has four electrons/Si, the "intercalated graphite" β-$ThSi_2$, and the twisted allotrope α-$ThSi_2$, both with six electrons/Si. A specific question was whether for this high electron count, and for the twisted structure, an interlayer band still exists at the Fermi level. This band is responsible for the superconductivity observed below ~10K in $4^1/_3$-electron graphites such as CaC_6. Here, the interlayer band couples to the π* band via C buckling and in-plane Ca modes, as has been understood from the ellipsoidal or toroidal shape of the Ca-centered Wannier orbital for the interlayer band. Also α- and β-$ThSi_2$ are superconducting, but only below 2−3 K. The problem is to disentangle the band structures, which are complicated due to the high electron count, the strong Th 6d character, and the cell doubling and twist for α-$ThSi_2$. For all cases, we found that a minimal *N*MTO basis with nine orbitals per $ThSi_2$, that is, merely three orbitals more than there are electron pairs, could accurately describe the occupied part of the band structure. This basis contains the six Si sp^2 orbitals, the two Si $p_\perp$ orbitals, and the Th s orbital. All other characters are downfolded. The Th s orbital, in particular, has Th 6d character downfolded, and we found it to be torus-shaped like the Ca-centered Wannier function in CaC_6. In the twisted α structure, the interlayer (Th s) orbitals is simply a twisted torus (Figures 6 and 12 or table of contents graphic). This suggests that the mechanism of superconductivity is the same as in the intercalated graphites. However, as seen from the disentangled band structures in Figures 7 and 13, the σ* band lies considerably lower in $ThSi_2$ than in the graphites, and since the filling is also higher, there are several σ* bands at the Fermi level. These partly gap the interlayer sheet of the Fermi surface and thereby weaken the interband mechanism. But by being strongly coupled via Si bond-stretching modes, the σ* bands presumably contribute an intraband mechanism similar to the one driving MgB_2 superconductivity below 40 K. The electronic density of states at the Femi level is 2 (β) to 3 (α) times those in CaC_6 and in MgB_2. Reasons why, then, $ThSi_2$ has such a low T_c may be the fractured bands near the Fermi level, the very different phonon spectrum, and many others. Detailed DFT phonon and electron−phonon calculations are clearly required.

We have also studied the bonding by constructing *N*MTO sets with merely as many orbitals as there are electron pairs, namely, six per formula unit. It was found that the bonding in both allotropes can be understood in the same way: Per formula unit, there are three weakened Si σ bonds, two Si $sp_\perp$ Th bonds, and a Si $p_\perp$ orbital binding weakly with Th. In the twisted structure, the bonding with Th is somewhat stronger.

Acknowledgment. E.Z. acknowledges financial support from the "International Max-Planck Research School for Advanced Materials" (IMPRS-AM). We thank A. Simon and H.-G. von Schnering for inspiring us to do this research and V. Antonov for performing calculations including spin−orbit coupling.